

# Data-Driven Feedforward Control for Trade-Off Optimization in Machine Stand Vibration Systems

1<sup>st</sup> Daigo Yamaguchi  
Dept. of Engineering  
Nagoya Institute of Technology  
Nagoya, Japan  
d.yamaguchi.619@stn.nitech.ac.jp

3<sup>rd</sup> Takuya Shiohara  
Dept. of Engineering  
Nagoya Institute of Technology  
Nagoya, Japan  
t.shiohara.562@nitech.jp

2<sup>nd</sup> Shota Teramoto  
Dept. of Engineering  
Nagoya Institute of Technology  
Nagoya, Japan  
s.teramoto.702@stn.nitech.ac.jp

4<sup>th</sup> Yoshihiro Maeda  
Dept. of Engineering  
Nagoya Institute of Technology  
Nagoya, Japan  
ymaeda@nitech.ac.jp

**Abstract**—In various industrial mechatronic equipment for processing and assembling electronic components, high-acceleration drives in the internal positioning mechanisms cause machine stand vibrations, degrading their production accuracy and throughput. Generally, a trade-off exists between the fast and precise control of positioning mechanisms and suppressing machine stand vibrations, which complicates control design. This study presents an extended data-driven vibration suppression feedforward (FF) control method that addresses both positioning performance and machine stand vibrations. The proposed method designs FF controllers to pursue the trade-off through a multi-objective optimization problem using predicted responses of both the positioning device and the machine stand. Experiments with a laboratory table positioning system demonstrate the effectiveness of the proposed method, compared to an existing data-driven vibration suppression FF control method.

**Index Terms**—Data-driven control, feedforward control, machine stand, vibration suppression, multi-objective optimization.

## I. INTRODUCTION

There is increasing demand for increased productivity in industrial mechatronics equipment, such as electronic component processing and assembling machines, thus making high-speed, high-precision control of internal positioning mechanisms a crucial challenge [1]. Such positioning mechanisms are mounted on a machine stand. When operated at high acceleration and deceleration, their reaction forces excite vibrations in the machine stand, deteriorating the positioning accuracy not only in the equipment itself, but also in neighboring equipment [2]. Therefore, fast and precise control of positioning mechanisms as well as suppressing machine stand vibrations are required. However, these goals involve a trade-off.

Various control approaches considering machine stand vibrations have been studied previously. For example,

acceleration feedback (FB) control [3],  $H_\infty$ -based FB control [4], and model-based feedforward (FF) control [5], [6] were explored. Among these approaches, model-based FF control enables more effective trade-off optimization for machine stand vibration systems, offering greater control performance than FB control. However, their performance strongly depends on the accuracy of system identification [7], and precise system identification generally requires considerable effort from engineers.

To address the challenges in control design, data-driven control, which eliminates the need for precise system identification, is a promising approach. The methods in [8], [9], [10] designed FF controllers to follow a set or shaped target position trajectory for a positioning device by solving a predicted response-based optimization problem, enabling vibration suppression in the controlled object when a non-vibrational target trajectory was provided. However, suppressing machine stand vibrations requires setting an appropriate trajectory before the FF controller design, and effective suppression is difficult without precise knowledge of machine stand vibrations. In contrast, data-driven vibration suppression control (DD-VSC) methods, e.g., [11] and [12], can suppress residual vibrations in both the positioning device and machine stand owing to their FF controller structure and optimization problem for vibration suppression. However, as the existing DD-VSC methods only predict the responses of positioning devices, they cannot suppress machine stand vibrations during positioning operations. To the best of the authors' knowledge, no data-driven FF control method effectively balances the trade-off in machine stand vibration systems.

This study presents an enhanced DD-VSC method, data-driven multi-objective VSC (DD-MOVSC) for fast and precise positioning in machine stand vibration systems. While the control design theory of DD-MOVSC is fundamentally based on the existing DD-VSC [11], [12], this study

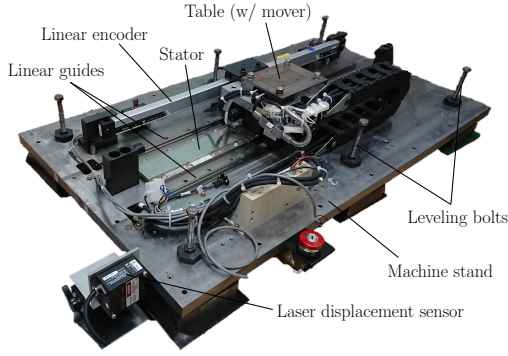


Fig. 1. The laboratory table positioning system.

extends it to design FF controllers through multi-objective optimization, incorporating the predicted responses of a machine stand by using an additional sensor on it to acquire learning data. Furthermore, DD-MOVSC easily balances the trade-off performance by a weighting coefficient. Experiments emulating machine stand vibration systems were conducted using a table positioning mechanism to validate its effectiveness compared to a standard DD-VSC method.

## II. PROBLEM STATEMENT

### A. Controlled Object

The appearance of the laboratory table positioning device used as the controlled object is shown in Fig. 1. This device was designed to emulate the precision positioning mechanism in electronic component processing machines. A moving table driven by a linear motor is mounted on a machine stand and guided by rolling ball guideways on the machine stand. The machine stand is kept on the floor with six leveling bolts and vibrates when the table operated at high acceleration and deceleration. The table position  $x_t$ , which is the relative displacement for the machine stand, is detected by a linear encoder mounted on the machine stand. The detected signal is fed back to control the table position through a prototyping controller (MicroLabBox, dSPACE) with a control period of  $T_s = 500 \mu s$  and a servo amplifier. The machine stand displacement  $x_{ms}$  on the floor is detected by a laser displacement sensor (LK-H025, LK-G5000, Keyence), which is used for the design of FF controllers in the DD-MOVSC and evaluation.

The measured frequency responses of the plant from the motor thrust reference  $u$  as the control input to  $x_t$  and  $x_{ms}$  are shown in Fig. 2. The resonance mode due to the machine stand exists approximately at 38 Hz. Additionally, in the low-frequency range, gain reduction and phase lead occur owing to the nonlinear friction generated at the linear guides [13].

The target control specification is to settle the table position within  $\pm 4 \mu m$  to the target position within 40 ms during a point-to-point positioning operation with a stroke of  $X_r = 1 \text{ mm}$ . Additionally, throughout the positioning operation, the machine stand vibration should be suppressed within  $\pm 15 \mu m$ .

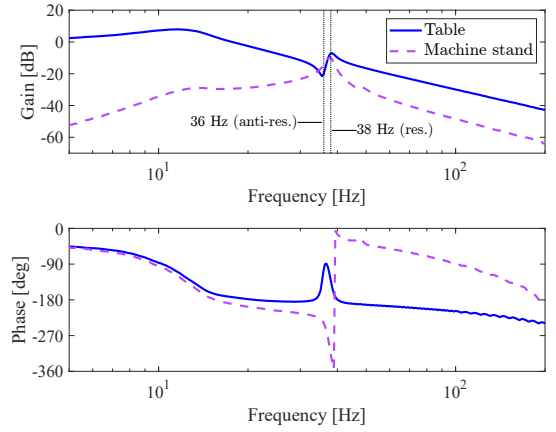


Fig. 2. Frequency characteristics of the plant.

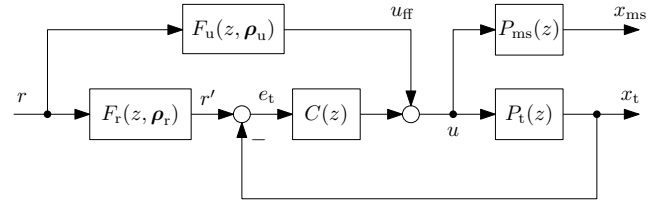


Fig. 3. Block diagram of the 2DoF positioning control system.

### B. Control Problem

The block diagram of the two-degree-of-freedom (2DoF) positioning control system considered in this study is shown in Fig. 3, where  $r$  is the position command for the table,  $r'$  is the table position trajectory reference,  $e_t$  is the table position tracking error,  $u_{ff}$  is the FF control input,  $P_t(z)$  represents the dynamics of the table,  $P_{ms}(z)$  represents the dynamics of the machine stand,  $C(z)$  represents the FB controller,  $F_r(z, \rho_r)$  and  $F_u(z, \rho_u)$  represent FF controllers with the parameter vectors  $\rho_r$  and  $\rho_u$  to be designed. The discrete-time transfer functions  $P_t(z)$  and  $P_{ms}(z)$  are defined as follows, neglecting the differences in sensor characteristics between the table and the machine stand, characteristics of the servo amplifier, friction, and disturbing noises for simplicity.

$$\begin{aligned} P_t(z) &= \frac{x_t(z)}{u(z)} = \frac{N_t(z)}{D_t(z)D(z)} \\ P_{ms}(z) &= \frac{x_{ms}(z)}{u(z)} = \frac{N_{ms}(z)}{D(z)} \end{aligned} \quad (1)$$

where  $N_t(z)$  and  $D_t(z)$  respectively represent the numerator and denominator polynomials in  $P_t(z)$ ;  $N_{ms}(z)$  represents the numerator polynomial in  $P_{ms}(z)$ ; and  $D(z)$  denotes the common denominator polynomial that includes poles due to the machine stand vibration.

The control problem is to design the FF controllers,  $F_r(z, \rho_r)$  and  $F_u(z, \rho_u)$ , to achieve the target control specification stated in Sect. II-A.  $F_r(z, \rho_r)$  and  $F_u(z, \rho_u)$  are designed in a data-driven manner using experimental data,  $x_t$  or  $x_{ms}$ , obtained from a single positioning operation. To satisfy the target control specifications,  $F_r(z, \rho_r)$  and  $F_u(z, \rho_u)$  that

can pursue a trade-off between the fast and precise positioning of the table and suppressing machine stand vibrations are required.

In this study, a discrete-time linear time-invariant system  $G$  with input  $v(n)$  and output  $y(n)$  ( $n$  denotes the discrete-time index) is defined in the lifted system representation as:

$$\mathbf{y} = \mathbf{G}\mathbf{v} \quad (2)$$

with

$$\begin{aligned} \mathbf{y} &= [y(0) \ y(1) \ \cdots \ y(N-1)]^\top \in \mathbb{R}^N \\ \mathbf{v} &= [v(0) \ v(1) \ \cdots \ v(N-1)]^\top \in \mathbb{R}^N \\ \mathbf{G} &= \begin{bmatrix} D_G & 0 & \cdots & 0 \\ C_G B_G & D_G & \cdots & 0 \\ \vdots & \vdots & \ddots & \vdots \\ C_G A_G^{N-2} B_G & C_G A_G^{N-3} B_G & \cdots & D_G \end{bmatrix} \in \mathbb{R}^{N \times N} \end{aligned} \quad (3)$$

where,  $A_G$ ,  $B_G$ ,  $C_G$ , and  $D_G$  are the coefficient matrices of the state-space representation of  $G$ .

### III. DD-VSC

In this section, we briefly describe a theoretical formulation of the data-driven optimization problem in the conventional DD-VSC method [11], [12], and then, theoretically analyze the characteristics of DD-VSC for machine stand vibration systems.

#### A. Optimization Problem

The FF controllers,  $F_r(z, \rho_r)$  and  $F_u(z, \rho_u)$ , are defined as:

$$\begin{aligned} F_r(z, \rho_r) &= \Psi(z) \rho_r^\top \\ F_u(z, \rho_u) &= \Psi(z) \rho_u^\top \end{aligned} \quad (4)$$

with

$$\begin{aligned} \Psi_m(z) &= Q(z)z^{-m} \\ \Psi(z) &= [\Psi_0(z) \ \Psi_1(z) \ \cdots \ \Psi_M(z)] \in \mathbb{C}^{1 \times (M+1)} \\ \rho_r &= [\rho_{r0} \ \rho_{r1} \ \cdots \ \rho_{rM}] \in \mathbb{R}^{1 \times (M+1)} \\ \rho_u &= [\rho_{u0} \ \rho_{u1} \ \cdots \ \rho_{uM}] \in \mathbb{R}^{1 \times (M+1)} \\ \rho &= [\rho_r \ \rho_u] \in \mathbb{R}^{1 \times 2(M+1)} \end{aligned} \quad (5)$$

where  $\Psi_m(z)$ ,  $m \in \{0, 1, \dots, M\}$  denote the basis functions including an arbitrary, stable filter  $Q(z)$ . DD-VSC designs the FF controllers by solving an optimization problem based on the predicted table position responses. The optimization problem is defined as:

$$\begin{aligned} \min_{\rho} \quad & \mathcal{J}_t(\rho) \\ \text{s.t.} \quad & \Gamma_r \rho^\top = 1 \end{aligned} \quad (6)$$

with

$$\begin{aligned} \mathcal{J}_t(\rho) &= \|\hat{e}_t(\rho)\|_2 \\ \hat{e}_t(\rho) &= [\hat{e}_t(0, \rho) \ \hat{e}_t(1, \rho) \ \cdots \ \hat{e}_t(N-1, \rho)]^\top \in \mathbb{R}^N \end{aligned} \quad (7)$$

$$\Gamma_r = [1 \ 1 \ \cdots \ 1 \ \mathbf{O}_{1 \times (M+1)}]^\top \in \mathbb{R}^{2(M+1)}$$

Here,  $\hat{e}_t(n, \rho)$ ,  $n \in \{0, 1, \dots, N-1\}$  represent the predicted table position tracking errors and  $\mathcal{J}_t(\rho)$  is the performance cost function for the table. In contrast, the equality constraint is introduced to ensure  $r' = r$  in the steady state.

#### B. Prediction of Table Responses

The actual table position tracking error  $e_t(n, \rho)$  over  $n \in \{0, 1, \dots, N-1\}$  in Fig. 3 is expressed as follows in the lifted system representation:

$$\begin{aligned} \mathbf{e}_t(\rho) &= [e_t(0, \rho) \ e_t(1, \rho) \ \cdots \ e_t(N-1, \rho)]^\top \\ &= (\mathbf{I} + \mathbf{P}_t \mathbf{C})^{-1} \mathbf{P}_t (\mathbf{C} \mathbf{F}_r(\rho_r) + \mathbf{F}_u(\rho_u)) \mathbf{r} \end{aligned} \quad (8)$$

with

$$\mathbf{r} = [r(0) \ r(1) \ \cdots \ r(N-1)]^\top \in \mathbb{R}^N \quad (9)$$

where  $\mathbf{P}_t \in \mathbb{R}^{N \times N}$ ,  $\mathbf{C} \in \mathbb{R}^{N \times N}$ ,  $\mathbf{F}_r(\rho_r) \in \mathbb{R}^{N \times N}$ , and  $\mathbf{F}_u(\rho_u) \in \mathbb{R}^{N \times N}$  are the matrices corresponding to  $P(z)$ ,  $C(z)$ ,  $F_r(z, \rho_r)$ , and  $F_u(z, \rho_u)$ , respectively. To predict  $\hat{e}_t(n, \rho)$  without requiring precise knowledge for the plant, such as mathematical models, experimental data for  $r$  and  $x_t$  are preliminary collected as the learning data. These learning data are acquired by conducting a positioning experiment with initial parameter vectors  $\rho_r^{\text{ini}}$  and  $\rho_u^{\text{ini}}$  for the FF controllers and expressed as:

$$\begin{aligned} \mathbf{r}^{\text{lrn}} &= [r^{\text{lrn}}(0) \ r^{\text{lrn}}(1) \ \cdots \ r^{\text{lrn}}(N-1)]^\top \in \mathbb{R}^N \\ \mathbf{x}^{\text{lrn}} &= [x^{\text{lrn}}(0) \ x^{\text{lrn}}(1) \ \cdots \ x^{\text{lrn}}(N-1)]^\top \in \mathbb{R}^N \end{aligned} \quad (10)$$

By using the learning data in (10),  $\hat{e}_t(n, \rho)$  is obtained as follows in a data-driven manner [12], [14]:

$$\begin{aligned} \hat{e}_t(\rho) &= \mathbf{F}_r(\rho_r) \mathbf{r} - \hat{\mathbf{T}}_t (\mathbf{C} \mathbf{F}_r(\rho_r) + \mathbf{F}_u(\rho_u)) \mathbf{r} \\ &= [(\mathbf{I} - \hat{\mathbf{T}}_t \mathbf{C}) \Psi_r \quad -\hat{\mathbf{T}}_t \Psi_u] \rho^\top = \Sigma_t \rho^\top \end{aligned} \quad (11)$$

with

$$\begin{aligned} \hat{\mathbf{T}}_t &= \mathbf{X}_t^{\text{lrn}} \{(\mathbf{C} \mathbf{F}_r(\rho_r^{\text{ini}}) + \mathbf{F}_u(\rho_u^{\text{ini}})) \mathbf{R}^{\text{lrn}}\}^{-1} \in \mathbb{R}^{N \times N} \\ \Psi_r &= [\Psi_0 \mathbf{r} \ \Psi_1 \mathbf{r} \ \cdots \ \Psi_M \mathbf{r}] \in \mathbb{R}^{N \times (M+1)} \end{aligned} \quad (12)$$

Here,  $\mathbf{R}^{\text{lrn}}$  and  $\mathbf{X}_t^{\text{lrn}}$  represent the Toeplitz matrices respectively defined using  $\mathbf{r}^{\text{lrn}}$  and  $\mathbf{x}_t^{\text{lrn}}$ , whereas  $\Psi_m \in \mathbb{R}^{N \times N}$ ,  $m \in \{0, 1, \dots, M\}$  are the matrices corresponding to  $\Psi_m(z)$  in (5). Therefore, the table-performance cost  $\mathcal{J}_t(\rho)$  in (7) is defined using (11) and (12), and the solution of the optimization problem in (6) can be analytically obtained by the Lagrange multiplier method.

### C. Trade-Off Characteristics

In DD-VSC, when the optimal parameter vector  $\rho^*$  ideally offering  $e_t = 0$  is obtained, the transfer characteristics from  $r$  to  $x_t$  and  $x_{ms}$  in Fig. 3 are formulated as [7]:

$$\begin{aligned} \frac{x_t(z, \rho^*)}{r(z)} &= N_t(z) F^{\text{red}}(z, \rho^*) Q(z) \\ \frac{x_{ms}(z, \rho^*)}{r(z)} &= N_{ms}(z) D_t(z) F^{\text{red}}(z, \rho^*) Q(z) \end{aligned} \quad (13)$$

where  $F^{\text{red}}(z)$  is the redundant polynomial when the order of the FF controllers is bigger than that of  $P_t(z)$ . From (13), both the table and machine stand have response poles arbitrarily defined by  $Q(z)$ , which allows DD-VSC to suppress the vibrations of both the table and the machine stand at the settling region in the table positioning operation. However, during the transient region, the control input for positioning the table excites the machine stand, which cannot be avoided inherently. It seems possible to optimize the trade-off by appropriately designing  $Q(z)$ ; however, this would require detailed plant information.

### IV. DD-MOVSC

To efficiently optimize the trade-off in machine stand vibration systems, we propose DD-MOVSC by extending the conventional DD-VSC to a method of designing FF controllers through a multi-objective optimization. The predicted machine stand responses are considered by introducing an additional sensor for the machine stand.

#### A. Optimization Problem

In DD-MOVSC, the FF controllers are identical to those of DD-VSC defined in (4) and (5), and designed by solving the following multi-objective optimization problem considering not only the table position but also the machine stand displacement:

$$\begin{aligned} \min_{\rho} \quad & \mathcal{J}_t(\rho) + \alpha \mathcal{J}_{ms}(\rho) \\ \text{s.t.} \quad & \mathbf{\Gamma}_r \rho^\top = 1 \end{aligned} \quad (14)$$

with

$$\begin{aligned} \mathcal{J}_{ms}(\rho) &= \|\hat{\mathbf{x}}_{ms}(\rho)\|_2 \\ \hat{\mathbf{x}}_{ms}(\rho) &= \begin{bmatrix} \hat{x}_{ms}(0, \rho) & \hat{x}_{ms}(1, \rho) \\ \cdots & \hat{x}_{ms}(N-1, \rho) \end{bmatrix}^\top \in \mathbb{R}^N \end{aligned} \quad (15)$$

where  $\mathcal{J}_{ms}(\rho)$  represents the additional performance cost for the machine stand,  $x_{ms}(n, \rho)$ ,  $n \in \{0, 1, \dots, N-1\}$  denote the predicted displacement of the machine stand, and  $\alpha \in \mathbb{R}_{\geq 0}$  is the weighting coefficient determining the balance of the trade-off.

When  $\alpha = 0$ , DD-MOVSC is equivalent to DD-VSC, such that  $x_t$  and  $x_{ms}$  are determined by (13), resulting in  $e_t = 0$ . However, when designed under  $\alpha > 0$ , the FF controllers are designed to minimize the weighted sum of the performance costs for both the table and machine stand. Therefore, although DD-MOVSC requires adding a sensor to the machine stand to

acquire the learning data for  $x_{ms}$ , it is expected to pursue the trade-off more effectively than DD-VSC.

#### B. Prediction of Machine Stand Responses

Similar to predicting the table responses described in Sect. III-B, the machine stand displacement  $x_{ms}(n, \rho)$  in Fig. 3 is performed by using the learning data for  $x_{ms}$ . The actual machine stand displacement  $x_{ms}(n, \rho)$  over  $n \in \{0, 1, \dots, N-1\}$  is formulated as:

$$\begin{aligned} \mathbf{x}_{ms}(\rho) &= \begin{bmatrix} x_{ms}(0, \rho) & x_{ms}(1, \rho) \\ \cdots & x_{ms}(N-1, \rho) \end{bmatrix}^\top \\ &= (\mathbf{I} + \mathbf{P}_t \mathbf{C})^{-1} \mathbf{P}_{ms} (\mathbf{C} \mathbf{F}_r(\rho) + \mathbf{F}_r(\rho)) \mathbf{r} \end{aligned} \quad (16)$$

where  $\mathbf{P}_{ms} \in \mathbb{R}^{N \times N}$  is the matrix corresponding to  $P_{ms}(z)$ . Additionally, the learning data  $x_{ms}^{\text{lrn}}$  obtained from a preliminary positioning experiment with  $\rho_r^{\text{ini}}$  and  $\rho_u^{\text{ini}}$  is formulated as:

$$\mathbf{x}_{ms}^{\text{lrn}} = \begin{bmatrix} x_{ms}^{\text{lrn}}(0) & x_{ms}^{\text{lrn}}(1) & \cdots & x_{ms}^{\text{lrn}}(N-1) \end{bmatrix}^\top \in \mathbb{R}^N \quad (17)$$

By using (16) and (17), the predicted machine stand displacement  $\hat{x}_{ms}(n, \rho)$  is expressed as follows:

$$\begin{aligned} \hat{\mathbf{x}}_{ms}(\rho) &= \hat{\mathbf{T}}_{ms} (\mathbf{C} \mathbf{F}_r(\rho_r) + \mathbf{F}_u(\rho_u)) \mathbf{r} \\ &= \begin{bmatrix} \hat{\mathbf{T}}_{ms} \mathbf{C} \mathbf{\Psi}_r & \hat{\mathbf{T}}_{ms} \mathbf{\Psi}_r \end{bmatrix} \rho^\top = \Sigma_{ms} \rho^\top \end{aligned} \quad (18)$$

with

$$\hat{\mathbf{T}}_{ms} = \mathbf{X}_{ms}^{\text{lrn}} \{ (\mathbf{C} \mathbf{F}_r(\rho_r^{\text{ini}}) + \mathbf{F}_u(\rho_u^{\text{ini}})) \mathbf{R}^{\text{lrn}} \}^{-1} \in \mathbb{R}^{N \times N} \quad (19)$$

where  $\mathbf{X}_{ms}^{\text{lrn}} \in \mathbb{R}^{N \times N}$  denotes the Toeplitz matrix defined using  $\mathbf{x}_{ms}^{\text{lrn}}$  in (17).

#### C. Solution Calculation

The objective function in (14) is formulated as follows, by using (11) and (18):

$$\mathcal{J}_t(\rho) + \alpha \mathcal{J}_{ms}(\rho) = \rho (\Sigma_t^\top \Sigma_t + \alpha \Sigma_{ms}^\top \Sigma_{ms}) \rho^\top \quad (20)$$

Therefore, the solution  $\rho^*$  of the constrained, multi-objective optimization problem in (14) can be obtained as (21), based on the Lagrange multiplier method.

$$\begin{aligned} \rho^{*\top} &= \left\{ \mathbf{\Gamma}_r (\Sigma_t^\top \Sigma_t + \alpha \Sigma_{ms}^\top \Sigma_{ms})^{-1} \mathbf{\Gamma}_r^\top \right\}^{-1} \\ &\quad (\Sigma_t^\top \Sigma_t + \alpha \Sigma_{ms}^\top \Sigma_{ms})^{-1} \mathbf{\Gamma}_r^\top \end{aligned} \quad (21)$$

From the above design theory, DD-MOVSC easily balances the trade-off between the table positioning performance and the machine stand vibrations by the weighting factor  $\alpha$ .

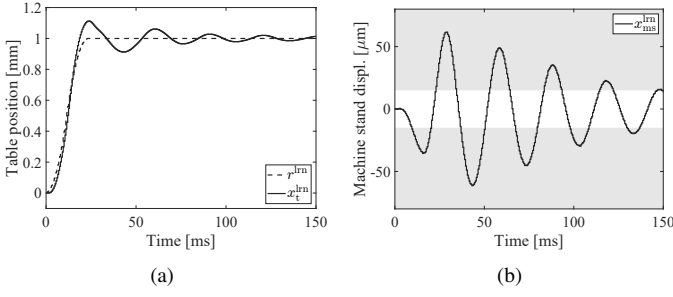


Fig. 4. Response waveforms of the positioning experiment for learning data acquisition: (a) position command  $r^{\text{lrn}}$  and table position  $x_t^{\text{lrn}}$ ; (b) machine stand displacement  $x_{\text{ms}}^{\text{lrn}}$ .

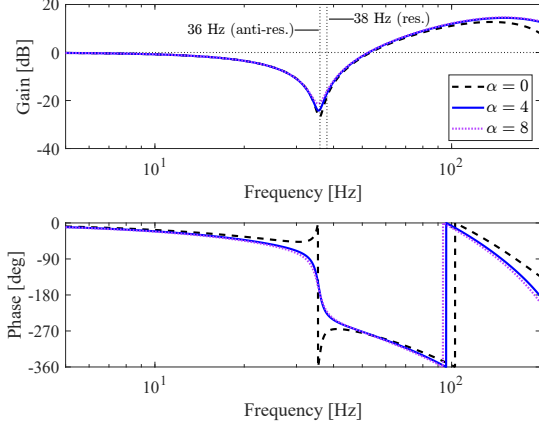


Fig. 5. Frequency characteristics of  $F_r(z)$ .

## V. EXPERIMENTAL EVALUATION

### A. Experimental Conditions

The positioning experiments were performed using the 2DoF control system shown in Fig. 3. The FB controller  $C(z)$  was designed as a PID controller, with parameters tuned to ensure robust stability of the FB control system and low sensitivity in the low-frequency range [15]. The position command  $r$  for the table was set as an S-shaped command with a stroke of  $X_r = 1$  mm and settling time of 23 ms.

For the FF controllers,  $F_r(z, \rho_r)$  and  $F_u(z, \rho_u)$ , which aim to achieve trade-off optimization in the machine stand vibration system, the basis functions  $\Psi(z)$  were defined as follows with a low-pass filter  $Q(z)$ :

$$\Psi(z) = Q(z) \begin{bmatrix} 1 & z^{-1} & \dots & z^{-12} \end{bmatrix} \in \mathbb{C}^{1 \times 13} \quad (22)$$

$$Q(z) = \left\{ \frac{(1 - e^{-\omega_Q T_s})z}{z - e^{-\omega_Q T_s}} \right\}^2$$

where the cutoff frequency of  $Q(z)$  was set to  $\omega_Q = 2\pi \cdot 150$  rad/s to ensure that  $r'$  reaches near the target position within the target settling time. The orders of the basis function and the low-pass filter were determined through a trial-and-error process while evaluating the predicted response characteristics.

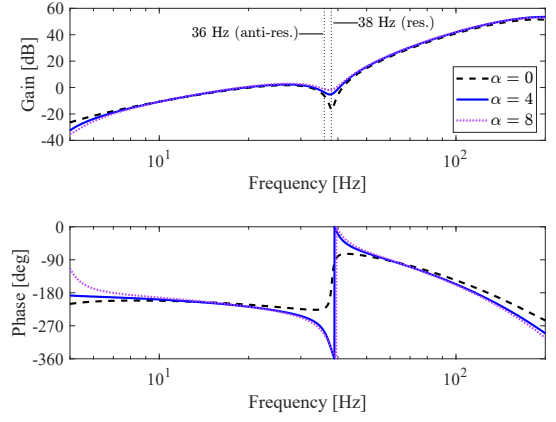


Fig. 6. Frequency characteristics of  $F_u(z)$ .

The learning data,  $x_t^{\text{lrn}}$ ,  $x_{\text{ms}}^{\text{lrn}}$ , and  $r^{\text{lrn}}$ , were acquired by conducting a single positioning experiment using the one-degree-of freedom control system, i.e.,  $F_r(z, \rho_r^{\text{ini}}) = 1$  and  $F_u(z, \rho_u^{\text{ini}}) = 0$  in Fig. 3. The response waveforms of the learning data are shown in Fig. 4. The length of the learning data was set to  $N = 800$  ( $NT_s = 400$  ms) and response predictions were performed in the time period  $n \in \{0, 1, \dots, N - 1\}$ .

### B. FF Controller Characteristics

The frequency characteristics of the FF controllers  $F_r(z)$  and  $F_u(z)$ , designed using DD-MOVSC with the weight  $\alpha = 0, 4$ , and  $8$ , are shown in Fig. 5 and Fig. 6, respectively. Note that  $\alpha = 0$  in DD-MOVSC corresponds to the standard DD-VSC introduced in Sect. III. For all  $\alpha$  conditions,  $F_r(z)$  reduces the gain near the anti-resonant frequency approximately at 36 Hz in the table dynamics depicted in Fig. 2, whereas  $F_u(z)$  reduces the gain near the resonant frequency approximately at 38 Hz in both the table and machine stand dynamics depicted in Fig. 2. In contrast, in the cases of  $\alpha = 4$  and  $\alpha = 8$ , both  $F_r(z)$  and  $F_u(z)$  exhibit phase changes around the frequencies near the vibration mode.

### C. Experimental Results

The experimental results of the positioning motion with  $\alpha = 0, 4$ , and  $8$  in DD-MOVSC are shown in Fig. 7. In the case of  $\alpha = 0$  corresponding to the standard DD-VSC, the table position satisfied the target control specifications. However, owing to the table positioning operation with the main response frequency of approximately 25 Hz, the machine stand vibrations slightly exceeded the target accuracy of  $\pm 15$   $\mu\text{m}$  during the transient response period of the table. As  $\alpha$  was increased to  $\alpha = 4$  and  $\alpha = 8$ , the table positioning performance deteriorated, whereas the machine stand vibrations during the transient response period were suppressed. Although the response characteristics of the table and machine stand varied with  $\alpha$ , the amplitude of the control input was kept within the limit of  $\pm 2$  V owing to the effect of  $Q(z)$ . To quantitatively compare the control performance with varying  $\alpha$ , Table I provides the maximum absolute table

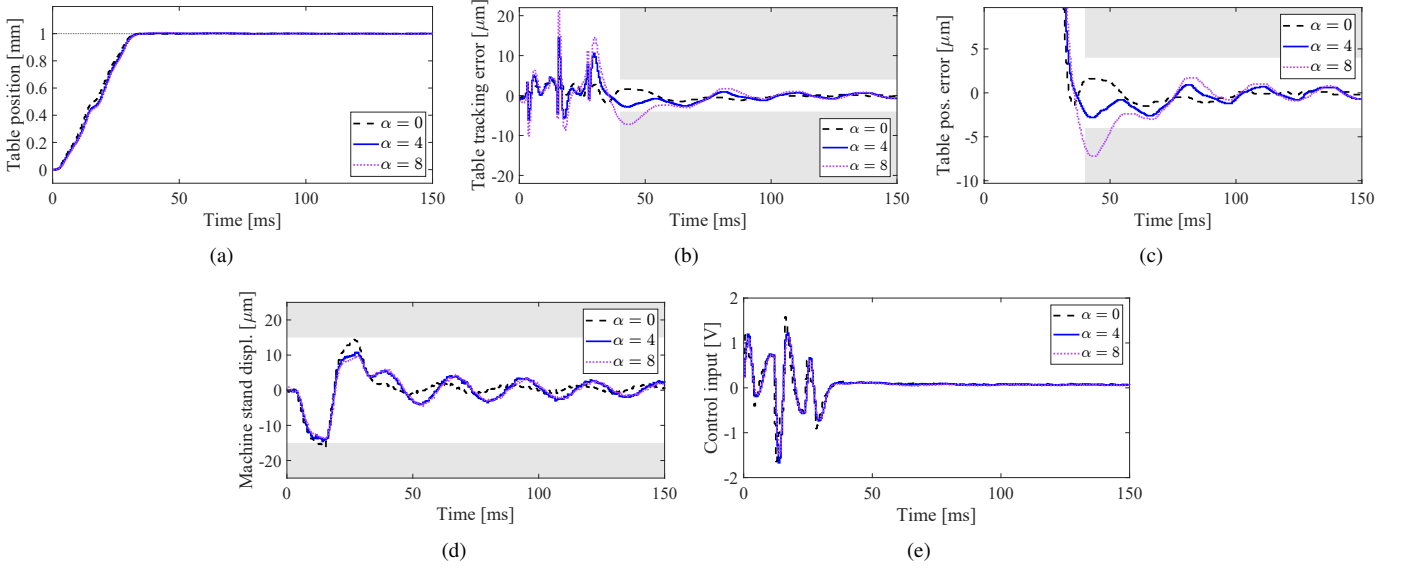


Fig. 7. Response waveforms of the positioning experiments by DD-MOVSC with varying weighting factor  $\alpha$ : (a) table position  $x_t$ , (b) table position tracking error  $e_t$ , (c) table position error  $X_r - x_t$ , (d) machine stand displacement  $x_{ms}$ , (e) control input  $u$ .

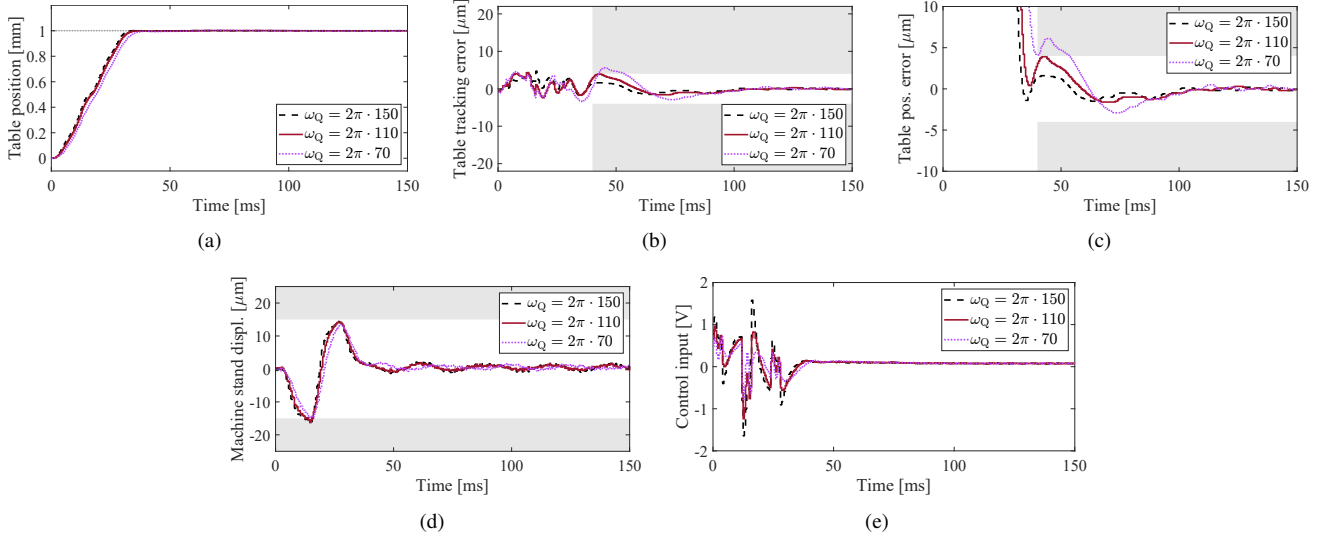


Fig. 8. Response waveforms of the positioning experiments by DD-VSC with varying cutoff frequency  $\omega_Q$ : (a) table position  $x_t$ , (b) table position tracking error  $e_t$ , (c) table position error  $X_r - x_t$ , (d) machine stand displacement  $x_{ms}$ , (e) control input  $u$ .

TABLE I  
QUANTITATIVE EVALUATION RESULTS OF CONTROL PERFORMANCE IN DD-MOVSC.

Weight $\alpha$	0	4	8
$\max( X_r - x_t )$ [um]	1.6	2.8	7.2
$\max( x_{ms} )$ [um]	16.3	14.6	13.7
$\sum e_t^2$ [um <sup>2</sup> ]	445.4	1594.1	4137.6
$\sum x_{ms}^2$ [um <sup>2</sup> ]	7648.9	7202.9	6014.6

position error  $|X_r - x_t|$ , maximum absolute machine stand displacement  $|x_{ms}|$ , sum of squared table position tracking errors  $e_t^2$ , and sum of squared machine stand displacements  $x_{ms}^2$ . The maximum absolute table position error was evaluated

after the target settling time of 40 ms, while the other metrics were evaluated over the time interval of  $[0, 150]$  ms. The results confirm that  $\alpha$  effectively adjusts the balance of the trade-off. In this study, when  $\alpha = 4$ , both the table and the machine stand satisfied the target control specifications.

To verify the effectiveness of DD-MOVSC in the trade-off optimization, the positioning experiments using the conventional DD-VSC, where the cutoff frequency  $\omega_Q$  in  $Q(z)$  was varied as  $\omega_Q = 2\pi \cdot 150$ ,  $2\pi \cdot 110$ , and  $2\pi \cdot 70$  rad/s at  $\alpha = 0$ , were conducted. The experimental results are shown in Fig. 8. As  $\omega_Q$  decreases, although the machine stand vibrations were suppressed, the table position responses were delayed. Consequently, it was not possible to find fine FF controllers that satisfy the target control specification. Fig. 9 illustrates the

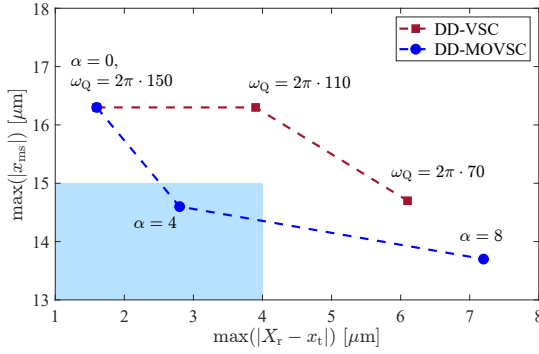


Fig. 9. Performance curves of DD-VSC and DD-MOVSC.

performance curves between  $\max(|X_r - x_t|)$  and  $\max(|x_{ms}|)$  for DD-VSC and DD-MOVSC. In Fig. 9, the blue area represents the region satisfying the target control specification. The DD-MOVSC outperforms the DD-VSC in the trade-off optimization capability, demonstrating its effectiveness for fast and precise positioning in machine stand vibration systems.

## VI. CONCLUSION

This paper presents a data-driven, multi-objective vibration-suppressing FF control method (DD-MOVSC) for high-speed and high-precision positioning in machine stand vibration systems. A key feature of DD-MOVSC is its ability to design FF controllers through trade-off optimization of the predicted responses of both the table and the machine stand, enabled by the integration of an additional sensor on the machine stand. The experimental results obtained from a laboratory table positioning mechanism with machine stand vibrations demonstrate that DD-MOVSC can effectively and efficiently achieve trade-off performance in machine stand vibration systems, outperforming the conventional DD-VSC method. Specifically, it achieved positioning control that meets the target specifications, with a table positioning accuracy of 2.8  $\mu\text{m}$  and machine stand vibration amplitude of 14.6  $\mu\text{m}$ .

Future research challenges include automating the design of the weighting factor  $\alpha$ , further pursuing the trade-off by optimizing the structure and parameters (such as  $\omega_Q$ ) of FF controllers, and theoretically establishing the conditions for learning data and each controller that enable parameter optimization based on (14).

## REFERENCES

- [1] Y. Maeda and M. Iwasaki, "Empirical transfer function estimation with differential filtering and its application to fine positioning control of galvano scanner," *IEEE Trans. Ind. Electron.*, vol. 70, no. 10, pp. 10466–10475, 2023.
- [2] S. Watanabe, R. Oguro, J. Kobayashi, and F. Ohkawa, "Modeling and position control based on a two-mass system for a machine stand vibration system," *J. Artificial Life Robotics*, vol. 11, no. 1, pp. 52–56, 2007.
- [3] T. Kai, H. Sekiguchi, and H. Ikeda, "Control structure with dual acceleration feedback for positioning machine with semi-closed servo system," *IEEE J. Ind. App.*, vol. 11, no. 2, pp. 351–358, 2022.
- [4] K. Ito, M. Iwasaki, and N. Matsui, "Robust fast and precise positioning of ball screw-driven table system on machine stand," in *Proc. IEEE Int. Workshop Adv. Motion Control*, 2004, pp. 511–515.
- [5] F. Terasaki, J. Kobayashi, R. Oguro, and F. Ohkawa, "A positioning control of a serial twin linear slider system with machine stand vibration," in *Proc. Int. Conf. Ind. Tech.*, 2006, pp. 2925–2930.
- [6] K. Ito and M. Iwasaki, "LMI-based command shaping approach considering interference between table systems," in *Proc. 5th IFAC Symp. Mechatron. Syst.*, 2010, pp. 194–199.
- [7] Y. Maeda and M. Iwasaki, "Improvement of adaptive property by adaptive deadbeat feedforward compensation without convex optimization," *IEEE Trans. Ind. Electron.*, vol. 62, no. 1, pp. 466–474, 2015.
- [8] S.H. van der Meulen, R.L. Tousain, and O.H. Bosgra, "Fixed structure feedforward controller design exploiting iterative trials: Application to a wafer stage and a desktop printer," *J. Dyn. Syst. Meas. Control.*, vol. 130, no. 5, 051006, 2008.
- [9] O. Kaneko and T. Nakamura, "Data-driven prediction of 2DOF control systems with updated feedforward controller," in *Proc. SICE Annu. Conf.*, 2017, pp. 259–262.
- [10] Y. Fujimoto, "Estimated response iterative tuning with signal projection," *IFAC J. Syst. Control*, vol. 19, 2022.
- [11] F. Boeren, D. Bruijnen, N. van Dijk, and T. Oomen, "Joint input shaping and feedforward for point-to-point motion: Automated tuning for an industrial nanopositioning system," *Mechatron.*, vol. 24, no. 6, pp. 572–581, 2014.
- [12] S. Teramoto, D. Yamaguchi, S. Sato, and Y. Maeda, "Data-driven feedforward control for suppressing coupled vibrations in positioning systems," in *Proc. IEEE Int. Conf. Mechatron.*, 2025.
- [13] Y. Maeda, K. Harata, and M. Iwasaki, "A friction model-based frequency response analysis for frictional servo systems," *IEEE Trans. Ind. Informat.*, vol. 14, no. 11, pp. 5246–5255, 2018.
- [14] Z. Zhang and W. Yin, "Data-driven feedforward control on active vibration isolation system," in *Proc. 17th Int. Conf. Control, Autom. and Syst.*, 2017, pp. 562–567.
- [15] E. Kuroda, Y. Maeda, and M. Iwasaki, "Efficient autonomous feedback controller parameter design considering robust stability for galvanometer scanner," *Electr. Eng. Jpn.*, vol. 215, no. 3, 2022.